Topographic organization of macaque area LIP

Gaurav H. Patel[a,b,c,d,1], Gordon L. Shulman[b], Justin T. Baker[c,e], Erbil Akbudak[a], Abraham Z. Snyder[a,b], Lawrence H. Snyder[c,2], and Maurizio Corbetta[a,b,c,2]

Departments of [a]Radiology, [b]Neurology, and [c]Anatomy and Neurobiology, Washington University, St. Louis, MO 63110; [d]Department of Psychiatry, Columbia University, New York, NY 10032; and [e]Department of Psychiatry, Massachusetts General Hospital, Boston, MA 02114

Edited by Michael Posner, University of Oregon, Eugene, OR, and approved January 7, 2010 (received for review July 20, 2009)

Despite several attempts to define retinotopic maps in the macaque lateral intraparietal area (LIP) using histological, electrophysiological, and neuroimaging methods, the degree to which this area is topographically organized remains controversial. We recorded blood oxygenation level–dependent signals with functional MRI from two macaques performing a difficult visual search task on stimuli presented at the fovea or in the periphery of the visual field. The results revealed the presence of a single topographic representation of the contralateral hemifield in the ventral subdivision of the LIP (LIPv) in both hemispheres of both monkeys. Also, a foveal representation was localized in rostral LIPv rather than in dorsal LIP (LIPd) as previous experiments had suggested. Finally, both LIPd and LIPv responded only to contralateral stimuli. In contrast, human studies have reported multiple topographic maps in intraparietal cortex and robust responses to ipsilateral stimuli. These blood oxygenation level–dependent functional MRI results provide clear evidence for the topographic organization of macaque LIP that complements the results of previous electrophysiology studies, and also reveal some unexpected characteristics of this organization that have eluded these previous studies. The results also delineate organizational differences between LIPv and LIPd, providing support for these two histologically defined areas may subserve different visuospatial functions. Finally, these findings point to potential evolutionary differences in functional organization with human posterior parietal cortex.

BOLD signal | functional MRI | retinotopy | parietal cortex | visual attention

The macaque lateral intraparietal area (LIP) has been the subject of many investigations over the past few decades. Anatomical studies of this area, which lies on the lateral bank of the intraparietal sulcus (IPS), have demonstrated widespread connectivity with a variety of cortical areas (1–3). Electrophysiological recordings in awake behaving macaques indicate that these connections underlie LIP's role in a range of functions ranging from the planning of saccades to the allocation of attention to the valuation of sensory information (4–6).

Despite the many studies of its functional and anatomical properties, the topographic organization of LIP remains controversial. Two electrophysiology studies have reported that LIP has a strong contralateral bias and may be retinotopically organized (3, 7). However, the maps in these studies were coarse and not consistent with one another. In contrast, another study found neither a retinotopic map nor a contralateral-hemifield bias (8). Electrical stimulation studies of LIP have also resulted in an unusual result: in both studies, the sites representing the horizontal meridian lie rostral to those representing both the lower and upper visual fields (9, 10). Thus, the issue of topography in LIP remains an open question.

Architectonic studies have divided LIP into dorsal and ventral divisions, but the functional significance of this difference is unclear (3, 11). Although cells throughout LIP appear to play a role in visual and oculomotor processing, the ventral subdivision of the LIP (LIPv) may be more involved in more complex cognitive functions compared with the dorsal subdivision of the LIP (LIPd) (6, 12, 13), and LIPd may be more involved in representing the fovea (3, 7, 14).

An alternative methodology to single unit recording is blood oxygenation level–dependent (BOLD) functional MRI (fMRI) (15–17). BOLD signals represent the integration of neural activity across millions of neurons. As a result, patterns of topography that are difficult to resolve at the single neuron scale may become clear with BOLD fMRI (18). However, BOLD signals may be driven more by synaptic and/or dendritic activity than action potentials, and therefore may produce different results from single unit recording (17, 19).

Recently, BOLD fMRI has been used to reveal topographic organization in the occipital cortices of monkeys passively viewing stimuli while fixating a central point (20, 21). Given LIP's role in more complex cognitive functions such as oculomotor planning and allocation of attention, however, delineating its topography may require an active task that engages these functions more than passive viewing. This has not yet been systematically attempted. However, in parietal areas 7a and DP, Siegel and coworkers have used a peripheral detection task to uncover topographic representations of the contralateral hemifield with intrinsic optical imaging (22–24).

In this study, we mapped the functional and topographic organization of macaque LIP using BOLD fMRI in two macaques performing a demanding rapid serial visual presentation (RSVP) search task. The task does not address the relative roles of LIP in oculomotor planning and the allocation of spatial attention. Instead, the task was designed to evoke a large and sustained response from LIP neurons using stimuli at distinct retinotopic locations. We quantified the degree to which LIP BOLD activity was driven by ipsilateral versus contralateral stimuli and determined whether monkey LIP contains continuous maps of contralateral visual space.

Results

To study the topographic properties of macaque LIPd and LIPv, we trained two monkeys to each perform two versions of a visual search task. In the first experiment, the monkey fixated a central point while a single RSVP stream appeared for 12 s at the fovea, the near periphery or the far periphery (Fig. 1*A*, single stream task; see Fig. S1 and Table S1 for behavior). The near peripheral streams were centered at 6.8° of eccentricity in one of six locations in the upper, middle, or lower parts of either the left or right visual field (polar angle task). The far peripheral streams were centered at 15.6° eccentricity in the upper left or right (eccentricity task). In the second experiment, two streams were shown simultaneously for 60 s, one on each side of the fixation point (Fig. 1*A*, two-stream task). In each case, the streams consisted of rapid sequential presentations of 42 different images in random order, sampled with replacement. A different image was designated as the target in each session and the monkey's task was to make a minimal hand movement when that target was detected.

Author contributions: G.H.P., G.L.S., L.H.S., and M.C. designed research; G.H.P. performed research; G.H.P., G.L.S., J.T.B., E.A., A.Z.S., L.H.S., and M.C. contributed new reagents/analytic tools; G.H.P., G.L.S., A.Z.S., L.H.S., and M.C. analyzed data; and G.H.P., G.L.S., L.H.S., and M.C. wrote the paper.

The authors declare no conflict of interest.

This article is a PNAS Direct Submission.

[1]To whom correspondence should be addressed. E-mail:gauravpatel@gmail.com.

[2]L.H.S., and M.C. contributed equally to this article.

This article contains supporting information online at www.pnas.org/cgi/content/full/0908092107/DCSupplemental.

www.pnas.org/cgi/doi/10.1073/pnas.0908092107

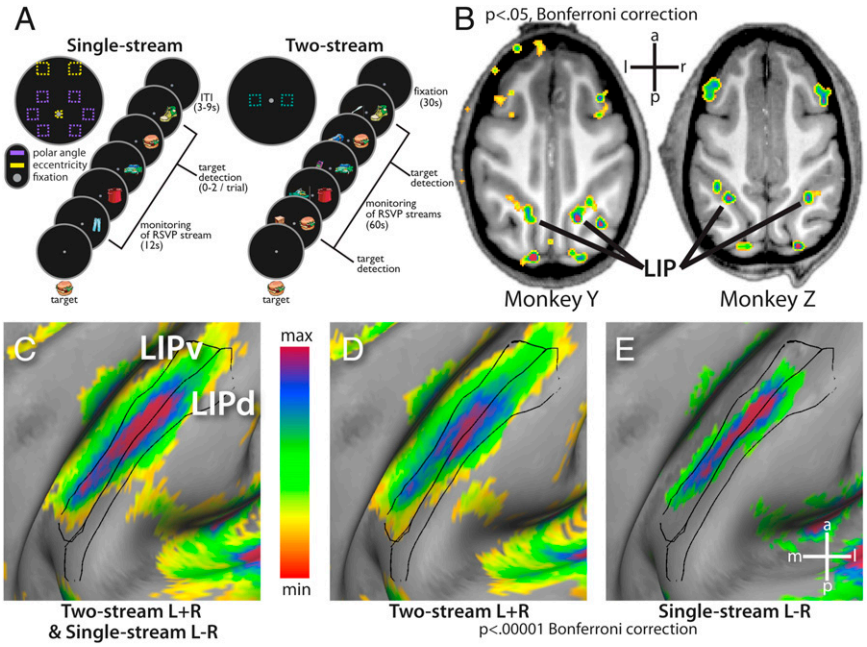

Fig. 1. Experimental paradigms and distribution of cortical activity in the single-stream polar angle and two-stream tasks. (*A*) the single stream paradigm and the two-stream paradigms and stimuli locations. (*B*) Horizontal slices through IPS in the two monkeys, demonstrating that the parietal foci in the conjunction map are centered on the lateral bank of the IPS in both monkeys. (*C–E*) A close-up of the inflated map projection of the fixed effects average of the single- and two-stream foci on the lateral bank of the IPS compared with the areal borders of LIPv and LIPd as defined by Lewis and Van Essen (11).

Functional Anatomy of RSVP Visual Search Tasks. We used general linear models (GLMs) to model the BOLD response to each of the six peripheral streams in the single-stream polar angle experiment, and the combined response to the streams in the two-stream experiment (see *SI Materials and Methods* for GLM details). The conjunction of maps from the two experiments (voxels significantly activated in the two-stream paradigm and with a significant contralateral bias in the single-stream paradigm) provided our regions of interest (ROIs). In this fixed-effects conjunction map (Fig. S2), we observed foci of BOLD signals in the retinotopically appropriate parts of visual cortex. Occipital foci were observed in the caudal portion of the calcarine sulcus, the posterior bank of the lunate sulcus, in the fundus of the inferior occipital sulcus, and on the gyral surface between the lunate and superior temporal sulci. When compared with previous histological, electrophysiological, and fMRI studies (20, 21, 25), these locations correspond to the representations of the horizontal meridian in V1, at the boundary between V2d and V3d, at the boundary between V2v and V3v/VP, and at the anterior boundary of V4, respectively (Fig. S3). BOLD signals in both experiments were also evoked in posterior parietal, inferotemporal, and prefrontal cortex (Fig. S2).

In posterior parietal cortex, a focus of activity spanned much of the lateral bank of the IPS from the fundus to the gyrus and stretched approximately 1cm in the axis parallel to the fundus, just anterior to the bend in the IPS (Fig. 1*B* and Fig. S2; activity thresholded at $P < 0.05$, Bonferroni corrected).

Using the CARET software package, the conjunction maps from each of the four hemispheres were projected to the macaque F6 atlas and compared to the Lewis and Van Essen histological atlas (11, 26) (*http://brainvis.wustl.edu*). This projection method uses anatomical markers to constrain the projection—no functional data from the current experiments were used. Fig. 1*D* shows that essentially all of histologically defined LIPv and two thirds of LIPd were activated in the two-stream task. In the one-stream task, more than two thirds of LIPv and one third of LIPd were activated (Fig. 1*E*). Thus, both bilateral and contralateral unilateral visual-field stimulation activate LIPd and LIPv (Fig. 1*C*). The activity evoked during the two-stream task subsumed the map of asymmetric activity evoked in the one-stream task. The greater extent of activation in the two-stream paradigm may have been due to a corresponding difference in power (i.e., BOLD signals in the single-stream paradigm were summed over 12 s of visual stimulation vs. 60 s in the two-stream paradigm). Alternatively, the greater activation in the two-stream task may reflect the greater attentional load resulting from the requirement to selectively focus attention on one of two identical visual streams. The results from each paradigm alone, however, still demonstrate that both bilateral and contralateral unilateral visual-field stimulation activates both LIPd and LIPv.

Contralateral Preference. From the LIP ROI in each hemisphere, we extracted the time course of the BOLD signal evoked by each of the six RSVP streams presented in the polar angle experiment. Fig. 2 shows that the three contralateral streams evoked a sustained 12-s response that was remarkably consistent across the three positions (solid red, blue, and green lines in Fig. 2), whereas the three ipsilateral responses were consistently flat or slightly negative (dotted lines in Fig. 2). A laterality index was defined as the difference in the mean magnitude of contralateral versus ipsilateral stream activity normalized by the mean contralateral stream magnitude [(contra-ipsi)/contra; *SI Materials and Methods*]. An index value near 0 corresponds to equivalent responses for contralateral and ipsilateral stimuli, a value near 1 corresponds to a strong bias toward contralateral stimuli with almost no response to ipsilateral stimuli, whereas a value significantly greater than 1 indicates a contralateral bias with ipsilateral suppression. The mean LIP laterality index across the four hemispheres was 1.17 (SEM, 0.14), similar to the index values in areas of visual cortex: 1.41 (0.23) for V1, 1.20 (0.29) for the V2d/V3d horizontal meridian, 0.97 (0.16) for the V2v/V3v horizontal meridian, and 1.11 (0.15) for V4 (Fig. S4). These results demonstrate that the BOLD response in LIP is completely lateralized, similar to those in early visual cortex areas.

The ROIs in this analysis were chosen to isolate voxels driven specifically by the visual stimulus, but they also bias the results toward finding lateralized responses. We therefore repeated the contralateral

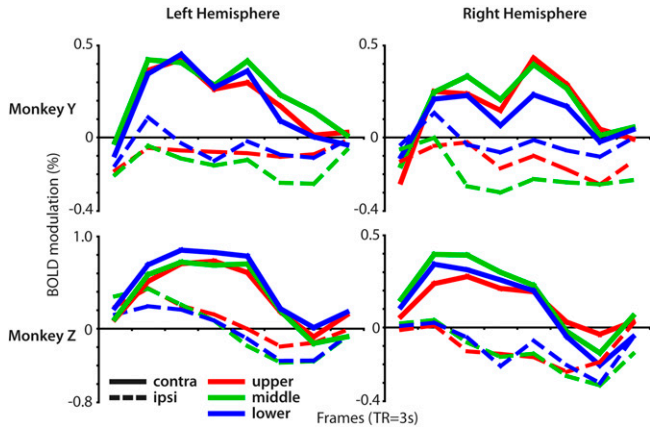

Fig. 2. Contralateral bias in LIP. (*A*) Time-courses of the BOLD signal in LIP in each of the four hemispheres evoked by the peripheral RSVP streams in the polar angle experiment. (*B*) The contralateral bias of LIP compared with occipital visual areas [index = (contra-ipsi)/contra; error bars reflect SEM].

index calculation with an ROI defined only by voxels significantly activated in the two-stream paradigm. Although the results were more variable across hemispheres, the mean LIP index value was still near 1 (1.41 (0.83)), which indicates that visually driven voxels in monkey LIP are activated primarily if not solely by contralateral stimuli.

Topographic Map of Contralateral Periphery. To test for a polar-angle map in LIP, we calculated a voxel-wise contrast of the activity evoked by each contralateral stream with the average activity evoked by the three ipsilateral streams (contra upper − [(ipsi upper + ipsi middle + ipsi lower) / 3]). This contrast isolated the BOLD signals related specifically to the presentation of each contralateral stream. The three maps from each individual hemisphere were projected to the macaque F6 right hemisphere surface and then thresholded to reveal the maxima ($P < 0.001$, uncorrected) on the lateral bank of the IPS (Fig. 3*A*). In all four hemispheres, the most reliable activity evoked by upper visual field stimulation was caudal to that of the lower visual field, and stimulation along the horizontal meridian was between the upper and lower field peaks. A fixed-effects average of the four hemispheres revealed a contiguous map of the contralateral peripheral visual field with an axis of organization that paralleled the fundus of the sulcus (Fig. 3*B*; $P < 0.05$ with Bonferroni correction). To confirm the existence of the map in a bias-free fashion and determine its statistical significance, a voxel-wise contrast was computed that directly compared the activity evoked by the contralateral upper and lower field streams for each hemisphere. The four contrast maps were combined in a fixed-effects average map (Fig. 3*C*) that showed the same topography as the maps in Fig. 3 *A* and *B*, indicating that the topographic organization was consistent across hemispheres ($P < 0.05$ with Bonferroni correction). No other candidate topographic maps were observed in the IPS of any of the four hemispheres.

To quantify the specificity of the topographic maps, the fixed-effects map of Fig. 3*B* was used to create ROIs for the upper, middle, and lower visual field representations. We then computed the magnitude of the activation evoked by each of the three contralateral streams relative to the average of the three ipsilateral streams within each ROI (Fig. 3*B Inset*). Our method of analysis guarantees that the activity for the upper stream will be largest for the upper ROI, activity for the middle stream will be largest for the middle ROI, and activity for the lower stream will be largest for the lower ROI. However, this quantification also reveals the specificity of these effects, e.g., whether and to what extent the upper stream also activates the middle and lower ROI. Furthermore, the same ROIs were used for all four hemispheres. The BOLD response in the upper field ROI (red) was eight times larger for the upper contralateral RSVP stream compared with the lower contralateral stream (0.72% vs. 0.09% modulation; $P < 0.01$). In contrast, the BOLD response in the lower field ROI (blue) was three times larger for the lower compared with the upper contralateral RSVP stream (0.75% vs. 0.25%; $P = 0.071$). These differences in the upper and lower field representations demonstrate that visual field location has a large and selective effect on LIP activation.

Periphery Versus Fovea. To investigate whether the fovea is represented separately from the periphery, we performed a second single-stream experiment in which the RSVP stream appeared randomly in one of three locations: at the fovea or in the upper field at 15° eccentricity and 18° to either the left or right of the vertical meridian. A GLM was used to create maps contrasting the activity evoked by each peripheral stream location versus the foveal stream for each monkey. For each hemisphere, the resulting contrast map was projected to the macaque F6 atlas and thresholded to isolate the peak positive (peripheral) and negative (foveal) areas on the lateral bank of the IPS ($P < 0.01$, uncorrected). In each of the four indi-

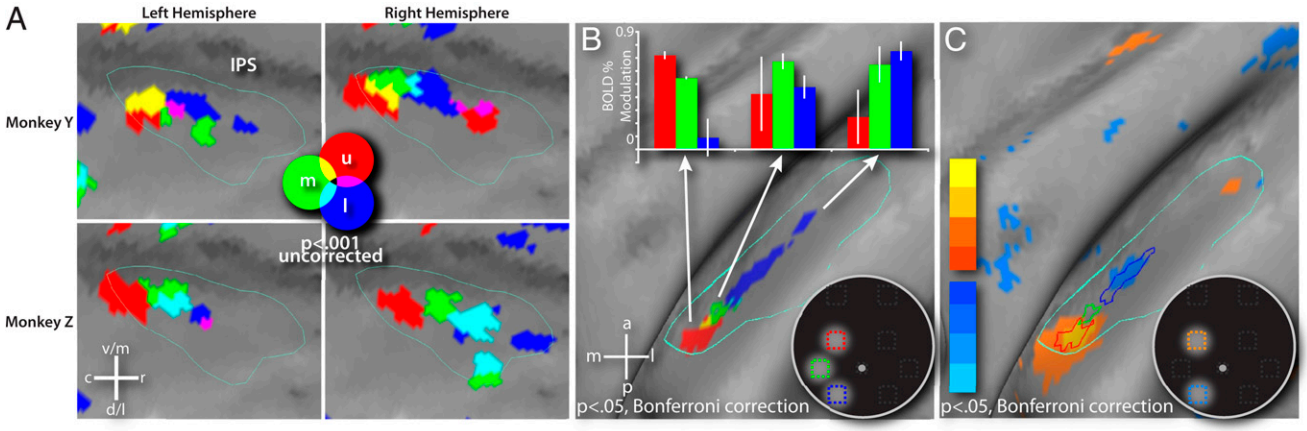

Fig. 3. Polar angle organization of LIP. (*A*) Close-up of LIP of each of the four hemispheres as projected to the macaque F6 atlas. The cyan border outlines LIP as defined by the conjunction in Fig. 1C, and the dark horizontal band in each image is the fundus of the IPS. The upper, middle, and lower fields are represented by red, green, and blue, respectively. Other colors represent the overlap of these representations. (*B*) Fixed-effects average of the LIP polar-angle map project on the inflated macaque F6 right hemisphere. Bar graph shows the magnitude of the activity evoked by the three contralateral RSVP streams for each part of the map (error bars reflect SEM). (*C*) Upper (yellow-orange) versus lower (blue) field contrast in LIP compared with the polar angle map from Fig. 3*B*.

vidual hemispheres, the contralateral peripheral stream representation was caudal to the foveal stream representation (Fig. 4*A*).

A group fixed-effects map created from the four hemisphere surface projections revealed two aspects of LIP organization (Fig. 4*B*; $P < 0.00001$, Bonferroni corrected). First, the 15° peripheral upper-field representation largely overlapped with the 7° upper field representation observed in the separate polar-angle experiment (red contour in Fig. 4*B*), confirming the overall reliability of the LIP topography discussed earlier. Second, the foveal representation was rostral and slightly ventral to the lower field representation (Fig. 4*B*). Fig. S5 demonstrates that the locations of these two representations are not dependent on the level of threshold. Within the peripheral representation, the difference in the magnitude of the activity evoked by the peripheral versus the foveal streams was 0.72% ± 0.31, and in the foveal representation this difference was –0.54% ± 0.25 (Fig. 4*B Inset*). These results indicate that foveal stimuli reliably activated a separate region within LIP rather than a region close to the confluence of the peripheral regions defined in the polar angle experiment.

Organization of LIP. To better understand the spatial relation of our results with the architectonic definitions of LIPd and LIPv, we compared the activation of LIP by the two-stream experiment (Fig. 5*A*), the topographic map derived from the single-stream experiment (Fig. 5*B*), and an objective probability map of the most likely locations of LIPd and LIPv derived from six hemispheres used in the Lewis and Van Essen study (Fig. 5*C*) (11). The most significant activations evoked by the two-stream experiment (purple and violet, Fig. 5*A*) are mostly within the borders of the "highest probability" LIPv (bright red, Fig. 5*C*) but with significant activation within LIPd (bright yellow, Fig. 5*C*). However, the topographic map evoked by the single-stream experiment is contained within the high-probability LIPv borders (compare Fig. 5*B* vs. Fig. 5*C*). Within these high-probability borders, LIPv demonstrated a greater preference for the contralateral field than LIPd that almost reached significance ($P = 0.073$, one-tailed paired t test, mean difference of 0.320 ± 0.164). However, the magnitude of activation evoked by the two-stream task was not greater in LIPv ($P = 0.195$, one-tailed paired t test).

Discussion

Using BOLD-fMRI in awake behaving macaques performing a demanding visual attention task, we have found that responses in monkey LIPd and LIPv overwhelmingly reflect visual stimuli in the contralateral hemifield, that LIPv may be more involved in the processing of contralateral stimuli than LIPd, and that in LIPv these responses are topographically organized. We also find evidence that the functionally and topographically derived borders of LIPv closely match those based on architectonic criteria.

We found no significant BOLD activity in LIP associated with ipsilateral stimuli in either voxel-wise maps or time-courses. This finding is consistent with most electrophysiological studies of LIP and with the strong contralateral bias reported in an fMRI study (3, 7, 27, 28; but see ref. 8). In contrast, fMRI studies in humans have demonstrated significant ipsilateral activity in parietal cortex in a variety of tasks (29–32). This difference may underlie a more profound difference in the organization and function of human and monkey IPS areas involved in visual attention and processing. However, the months of training received by monkeys compared with the few minutes of training often received by human subjects before testing could result in more extensive alteration of the monkey's cortical organization, and may also explain the cross-species difference in LIP laterality (33).

We found a topographic map of contralateral visual stimuli within the borders of LIPv (11). The upper visual field representation was located at the caudal end of LIPv, whereas the lower visual field was located more centrally. This is broadly consistent with a common interpretation of the findings of Ben Hamed et al. (7) but opposite to those of Blatt et al. (3). Both these studies found at best only coarse topographic organization, with many adjacent neurons violating the general trend and representing scattered parts of the visual field. Given the low-pass spatial filtering characteristics of fMRI compared with single unit recording, neurons with outlying receptive fields in a poorly organized topographic map would reduce the strength of the fMRI-derived map. Thus, the degree of topographic specificity that we observed was surprising. Previous neuroimaging studies of retinotopic organization have generally failed to elicit topographic maps in LIP using passive viewing of stimuli, although Fize et al. do report in one of four monkeys a caudal LIP polar angle map that is consistent with the one reported here (20, 21). The failure to consistently evoke this map fits the observation that the strongest responses in posterior parietal cortex are evoked by behaviorally relevant stimuli as opposed to passively viewed stimuli (4, 5, 34).

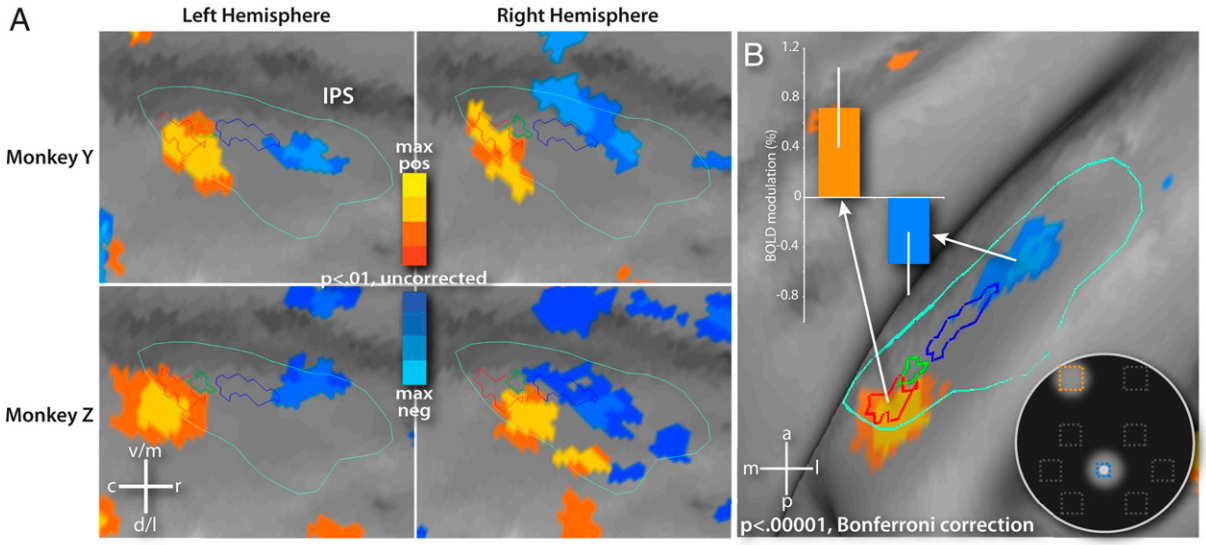

Fig. 4. Separation of peripheral and foveal representations in LIP compared with the polar angle map from Fig. 4*B*. (*A*) Close-up of LIP showing the peripheral (yellow-orange) and foveal (blue) representations in each of the four hemispheres. (*B*) Fixed-effects average of the LIP peripheral versus foveal stream contrast. Bar graph shows the difference in the evoked activity between the two streams for the two representations (error bars reflect SEM).

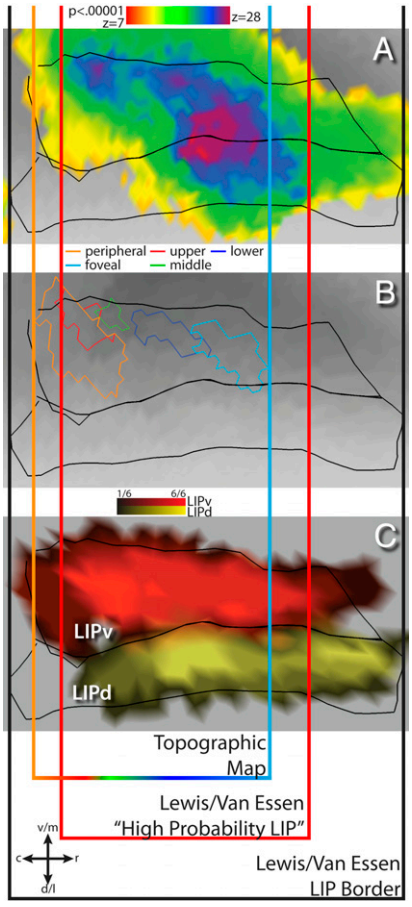

Fig. 5. Comparison of LIP visual activation, topography, and histological definition. Black outlines represent LIPd and LIPv borders from Lewis and Van Essen (11). Vertical lines demonstrate alignment between the three maps based on topographic and architectonic criteria. (*A*) Activation of LIPd and LIPv by the two-stream experiment (same as Fig. 1*D*). (*B*) Combination of polar angle and periphery versus fovea maps. (*C*) Probability map of the most likely locations of LIPd (yellow) and LIPv (red) from the Lewis and Van Essen study (11). Brighter colors indicate increased agreement about the location of the area among six of the hemispheres used in the study.

We also found a separate foveal representation in LIPv rostral to the peripheral field map. Previous electrophysiology studies placed the fovea dorsal to the peripheral field representation and concluded that LIP contained a coarse but contiguous retinotopic map of the contralateral field (3, 7, 14). However, our results are consistent with previous imaging studies reporting a rostral foveal representation (14, 21) and with LIP/frontal eye field (FEF) connectivity studies demonstrating that rostral LIP projects to the ventral portion of FEF representing the fovea/parafovea and caudal LIP to the dorsal portion of FEF representing the periphery (2, 35, 36). Differences between our results and those of the previous electrophysiology studies that used fixation to define the foveal representation in LIP may actually reflect a separation of neurons involved in fixation from those involved in the processing of foveal stimuli (14).

Finally, although the locations of the 15° and 7° representations suggest an eccentricity axis within LIPv, the representations were largely overlapping even though the visual stimuli did not overlap on the screen, which prevents a firm conclusion. As we were prevented by the magnet's bore from presenting stimuli at eccentricities >15°, our maps may not include portions of LIP representing these high eccentricities. However, the study of Ben Hamed et al. (7), which stimulated at eccentricities >20°, found that 76% of the mapped neurons had the center of their receptive fields at eccentricities <10°, indicating LIP may only poorly represent high-eccentricity portions of the visual field.

We find that distinct peripheral and foveal representations occur only within architectonically defined LIPv, and that LIPv may have a stronger contralateral preference than LIPd. In particular, the extent of visual activation and topographic organization agreed well with the area of increased myelination of layers 3 through 5 that defines LIPv (3, 11). Another recent imaging study found that LIPv was more strongly activated by memory-guided saccades, whereas both were activated by visually guided saccades (12). Other single-unit studies have reported that LIPv plays a role in integrating evidence during perceptual tasks (6). Finally, a recent lesion study shows that both LIPd and LIPv lesions affect visually guided and memory-guided saccades, whereas only LIPv lesions affect covert search (13). Taken together, the evidence suggests that LIPd may be involved in simple oculomotor behaviors whereas LIPv may be important for more complex tasks involving behaviorally relevant spatial representations.

All our results were remarkably reliable and consistent across four hemispheres of two macaques. The contralateral preference, polar angle map, and foveal/periphery distinction were highly significant in assumption-free voxel-wise contrasts after multiple comparisons correction in all four hemispheres. The maps were also stereotyped enough in location and orientation between hemispheres to allow for averaging after interhemispheric alignment based solely on the location of IPS and other sulci. This degree of stereotypy is notable given the degree of individual variation usually observed in human and monkey cortical organization (11, 37).

Human fMRI studies have reported multiple retinotopic maps in IPS with no separation between the periphery and fovea (31, 38–41). In contrast, our results indicate the presence of a single topographic map in macaque IPS. The increased number of maps in humans may reflect either the distribution of functions to multiple areas that were previously localized to a single cortical area in macaques, or the evolution of new functions requiring new topographic areas. Either possibility is consistent with the fact that parietal cortex in humans is much larger than in monkeys even after correcting for scale differences (42).

Topographic maps are likely to emerge from development or evolutionary processes that minimize connection distance between computational units for speed and energy/space efficiency (43–45). Thus, the degree of topographic mapping in a given area may reflect the degree to which computations in that area involve small regions of visual space, and the degree of lateralization may indicate the amount of computations involving information from both visual hemifields. For example, V1 is highly retinotopically organized and strongly lateralized, reflecting the local nature of neuronal interactions (46). The degree of topographic organization and laterality generally decreases in higher-level visual areas, reflecting increasing integration of information from larger portions of the visual field (31, 47, 48). Higher-order parietal and frontal areas that show weak topography are likely involved in the flexible and rapid association of inputs and outputs requiring communication between representations at arbitrary locations within visual space (49). Accordingly, the strong topography and contralateral biases observed in macaque LIP may indicate a stronger reliance on local interactions, and perhaps less flexibility in the ability to recombine information across the visual field or with other regions compared with human parietal cortex (50). Furthermore, the separation of the peripheral and foveal representations may be evidence of distinct computations occurring in those parts of the visual field.

In conclusion, this study supports a strong functional distinction between LIPv and LIPd, with the former area previously associated with more complex cognitive tasks also showing evidence of strong topographic organization. In addition to better targeting of future electrophysiological and anatomic studies, these results raise the possibility that the organization of human and macaque posterior

parietal areas may differ substantially. Hence, these potential interspecies differences should be taken into account when extrapolating electrophysiological data collected from monkeys to human models of visual processing and attention.

Materials and Methods

While the macaques performed the RSVP tasks, BOLD images were acquired in a 3-T Siemens Allegra MRI scanner. The images were corrected for motion and other artifacts through a series of automated image-processing programs, and were then analyzed with a GLM that separated the sustained response to the RSVP stream from other signals (eg, detection, reward). The resulting z-statistic maps were projected to flattened representations of the cortical surface created from each monkey's own anatomical images (CARET; *http://brainvis.wustl.edu*). These maps were then registered to a common atlas target available in CARET that contained LIP areal borders from the Lewis and Van Essen histological study (11). For more details, please the *SI Materials and Methods*.

ACKNOWLEDGMENTS. We thank Tom Malone, David Borton, Marcel Fremont, Jason Vytlacil, Matt Reiter, Erin Reid, Chad Sylvester, Anthony Jack, Giovanni D'Avossa, Carlo Sestieri, Mark McAvoy, Justin Vincent, John Harwell, Donna Dierker, David Van Essen, Marc Raichle, Steve Petersen, Leonardo Chelazzi, and Wim Vanduffel for aiding this study and for their comments on the manuscript. This study was supported by the McDonnell Center for Systems Neuroscience at Washington University, National Institute of Neurological Disease and Stroke Grants R01 NS48013 and F31 NS051972, National Institute of Mental Health (NIMH) Grant R01 MH71920-06, a European Union–funded Marie Curie Chair (MEXC-CT-2004-006783), National Eye Institute Grant R01 EY012135, the Washington University Silvio Conte Center (NIMH Grant MH-071616), and National Science Foundation (Integrative Graduate Education and Research Traineeship Program Grant 0548890).

1. Cavada C, Goldman-Rakic PS (1989) Posterior parietal cortex in rhesus monkey: I. Parcellation of areas based on distinctive limbic and sensory corticocortical connections. *J Comp Neurol* 287:393–421.
2. Lewis JW, Van Essen DC (2000) Corticocortical connections of visual, sensorimotor, and multimodal processing areas in the parietal lobe of the macaque monkey. *J Comp Neurol* 428:112–137.
3. Blatt GJ, Andersen RA, Stoner GR (1990) Visual receptive field organization and corticocortical connections of the lateral intraparietal area (area LIP) in the macaque. *J Comp Neurol* 299:421–445.
4. Bushnell MC, Goldberg ME, Robinson DL (1981) Behavioral enhancement of visual responses in monkey cerebral cortex. I. Modulation in posterior parietal cortex related to selective visual attention. *J Neurophysiol* 46:755–772.
5. Gnadt JW, Andersen RA (1988) Memory related motor planning activity in posterior parietal cortex of macaque. *Exp Brain Res* 70:216–220.
6. Shadlen MN, Newsome WT (2001) Neural basis of a perceptual decision in the parietal cortex (area LIP) of the rhesus monkey. *J Neurophysiol* 86:1916–1936.
7. Ben Hamed S, Duhamel JR, Bremmer F, Graf W (2001) Representation of the visual field in the lateral intraparietal area of macaque monkeys: a quantitative receptive field analysis. *Exp Brain Res* 140:127–144.
8. Platt ML, Glimcher PW (1998) Response fields of intraparietal neurons quantified with multiple saccadic targets. *Exp Brain Res* 121:65–75.
9. Thier P, Andersen RA (1998) Electrical microstimulation distinguishes distinct saccade-related areas in the posterior parietal cortex. *J Neurophysiol* 80:1713–1735.
10. Kurylo DD, Skavenski AA (1991) Eye movements elicited by electrical stimulation of area PG in the monkey. *J Neurophysiol* 65:1243–1253.
11. Lewis JW, Van Essen DC (2000) Mapping of architectonic subdivisions in the macaque monkey, with emphasis on parieto-occipital cortex. *J Comp Neurol* 428:79–111.
12. Bakola S, Gregoriou GG, Moschovakis AK, Savaki HE (2006) Functional imaging of the intraparietal cortex during saccades to visual and memorized targets. *Neuroimage* 31:1637–1649.
13. Liu YQ, Yttri EA and Snyder LH. Intention and Attention: Different functional roles for LIPd and LIPv. *Nature Neuroscience*, in press.
14. Ben Hamed S, Duhamel JR (2002) Ocular fixation and visual activity in the monkey lateral intraparietal area. *Exp Brain Res* 142:512–528.
15. Ogawa S, Lee TM, Kay AR, Tank DW (1990) Brain magnetic resonance imaging with contrast dependent on blood oxygenation. *Proc Natl Acad Sci USA* 87:9868–9872.
16. Bandettini PA, Wong EC, Hinks RS, Tikofsky RS, Hyde JS (1992) Time course EPI of human brain function during task activation. *Magn Reson Med* 25:390–397.
17. Logothetis NK, Pauls J, Augath M, Trinath T, Oeltermann A (2001) Neurophysiological investigation of the basis of the fMRI signal. *Nature* 412:150–157.
18. Logothetis NK (2008) What we can do and what we cannot do with fMRI. *Nature* 453:869–878.
19. Lauritzen M, Gold L (2003) Brain function and neurophysiological correlates of signals used in functional neuroimaging. *J Neurosci* 23:3972–3980.
20. Brewer AA, Press WA, Logothetis NK, Wandell BA (2002) Visual areas in macaque cortex measured using functional magnetic resonance imaging. *J Neurosci* 22:10416–10426.
21. Fize D, et al. (2003) The retinotopic organization of primate dorsal V4 and surrounding areas: A functional magnetic resonance imaging study in awake monkeys. *J Neurosci* 23:7395–7406.
22. Siegel RM, Raffi M, Phinney RE, Turner JA, Jandó G (2003) Functional architecture of eye position gain fields in visual association cortex of behaving monkey. *J Neurophysiol* 90:1279–1294.
23. Raffi M, Siegel RM (2005) Functional architecture of spatial attention in the parietal cortex of the behaving monkey. *J Neurosci* 25:5171–5186.
24. Raffi M, Siegel RM (2007) A functional architecture of optic flow in the inferior parietal lobule of the behaving monkey. *PLoS One* 2:e200.
25. Essen DC, Zeki SM (1978) The topographic organization of rhesus monkey prestriate cortex. *J Physiol* 277:193–226.
26. Van Essen DC (2002) Windows on the brain: the emerging role of atlases and databases in neuroscience. *Curr Opin Neurobiol* 12:574–579.
27. Koyama M, et al. (2004) Functional magnetic resonance imaging of macaque monkeys performing visually guided saccade tasks: comparison of cortical eye fields with humans. *Neuron* 41:795–807.
28. Barash S, Bracewell RM, Fogassi L, Gnadt JW, Andersen RA (1991) Saccade-related activity in the lateral intraparietal area. II. Spatial properties. *J Neurophysiol* 66:1109–1124.
29. Claeys KG, Lindsey DT, De Schutter E, Orban GA (2003) A higher order motion region in human inferior parietal lobule: evidence from fMRI. *Neuron* 40:631–642.
30. Medendorp WP, Goltz HC, Vilis T, Crawford JD (2003) Gaze-centered updating of visual space in human parietal cortex. *J Neurosci* 23:6209–6214.
31. Jack AI, et al. (2007) Changing human visual field organization from early visual to extra-occipital cortex. *PLoS One* 2:e452.
32. Serences JT, Boynton GM (2007) Feature-based attentional modulations in the absence of direct visual stimulation. *Neuron* 55:301–312.
33. Bichot NP, Schall JD, Thompson KG (1996) Visual feature selectivity in frontal eye fields induced by experience in mature macaques. *Nature* 381:697–699.
34. Robinson DL, Goldberg ME, Stanton GB (1978) Parietal association cortex in the primate: sensory mechanisms and behavioral modulations. *J Neurophysiol* 91:910–932.
35. Bullier J, Schall JD, Morel A (1996) Functional streams in occipito-frontal connections in the monkey. *Behav Brain Res* 76:89–97.
36. Bruce CJ, Goldberg ME, Bushnell MC, Stanton GB (1985) Primate frontal eye fields. II. Physiological and anatomical correlates of electrically evoked eye movements. *J Neurophysiol* 54:714–734.
37. Van Essen DC, Dierker DL (2007) Surface-based and probabilistic atlases of primate cerebral cortex. *Neuron* 56:209–225.
38. Konen CS, Kastner S (2008) Representation of eye movements and stimulus motion in topographically organized areas of human posterior parietal cortex. *J Neurosci* 28:8361–8375.
39. Silver MA, Ress D, Heeger DJ (2005) Topographic maps of visual spatial attention in human parietal cortex. *J Neurophysiol* 94:1358–1371.
40. Hagler DJ, Jr., Riecke L, Sereno MI (2007) Parietal and superior frontal visuospatial maps activated by pointing and saccades. *Neuroimage* 35:1562–1577.
41. Swisher JD, Halko MA, Merabet LB, McMains SA, Somers DC (2007) Visual topography of human intraparietal sulcus. *J Neurosci* 27:5326–5337.
42. Orban GA, Van Essen D, Vanduffel W (2004) Comparative mapping of higher visual areas in monkeys and humans. *Trends Cogn Sci* 8:315–324.
43. Klyachko VA, Stevens CF (2003) Connectivity optimization and the positioning of cortical areas. *Proc Natl Acad Sci USA* 100:7937–7941.
44. Kohonen T (1982) Self-organized formation of topologically correct feature maps. *Biol Cybern* 43:59–69.
45. Chklovskii DB, Koulakov AA (2004) Maps in the brain: what can we learn from them? *Annu Rev Neurosci* 27:369–392.
46. Callaway EM (1998) Local circuits in primary visual cortex of the macaque monkey. *Annu Rev Neurosci* 21:47–74.
47. Felleman DJ, Van Essen DC (1991) Distributed hierarchical processing in the primate cerebral cortex. *Cereb Cortex* 1:1–47.
48. Boussaoud D, Desimone R, Ungerleider LG (1991) Visual topography of area TEO in the macaque. *J Comp Neurol* 306:554–575.
49. Miller EK, Cohen JD (2001) An integrative theory of prefrontal cortex function. *Annu Rev Neurosci* 24:167–202.
50. Stoet G, Snyder LH (2007) Extensive practice does not eliminate human switch costs. *Cogn Affect Behav Neurosci* 7:192–197.